VHF DOPPLER RADAR BACKSCATTER MEASUREMENTS THROUGH THE ENTIRE NEUTRAL ATMOSPHERE (15-95 km) ABOVE JICAMARCA, PERU

C. R. Cornish*

School of Electrical Engineering
Cornell University
Ithaca, NY 14853

B. B. Balsley

NOAA/ERL/R445
Boulder, CO 80303

R. F. Woodman

Radio Observatorio de Jicamarca
Instituto Geofisico de Peru
Lima 100, Peru

For submission to Radio Science

*Present address: Space Physics Research Laboratory
University of Michigan
Ann Arbor, MI 48109-2143

Abstract

The Jicamarca 50-MHz radar was used to obtain backscattered echoes through the entire atmosphere (0-100 km). Previous radar observations at VHF have shown a gap near the 35-55 km region, where the lack of echoes is attributed to a lack of radar sensitivity. By using the full Jicamarca antenna array and maximum transmitter power and by optimizing transmitter duty cycle through the implementation of complementary codes, Doppler measurements display discernable peaks in the computed spectra from atmospheric signals in the gap region as well as above and below it.

The results indicate that a minimum power-aperture threshold in excess of 10^{10} W-m^2 is required in order to obtain backscatter echoes near 50 MHz through the entire neutral atmosphere.

The Mesospheric-Stratospheric-Tropospheric (MST) radar wind profiling technique has proved in recent years to be a useful tool to observe the dynamics of the lower to upper atmosphere. Using scatter from turbulent irregularities in the neutral atmosphere, the technique measures the Doppler shifts obtained from the backscattered echoes to determine the bulk motion of the atmosphere due to winds and waves. While radar backscatter echoes have been received from the troposphere and lower stratosphere (5-35 km) and the mid to upper mesosphere (55-90 km), a gap in backscattered signal power profiles, as first pointed out by Woodman and Guillen (1974), is observed in the intermediate regions of the middle atmosphere (35-55 km), where the weak signal returns from the atmosphere are obscured by receiver system noise.

For VHF radars, the lack of echoes from the gap region does not appear to be due to an absence of turbulent scatterers but rather to the lack of radar system sensitivity. Turbulent backscatter, the dominant scattering mechanism in the MST region at non-vertical elevation angles, occurs when turbulent irregularities exist at length scales corresponding to one-half the radar wavelength ($\lambda_{radar}/2$). In the lower neutral atmosphere scattering is due to fluctuations in density, temperature or, at the lowest altitudes, humidity. In the mesosphere, where the free electron density becomes appreciable, the scattering is due to irregularities, presumably driven by neutral turbulence, in an increasing gradient of electron density. Turbulent scattering theory assumes scattering from turbulent irregularities when the radar half-wavelength lies between λ_{min} and λ_{max}, where these quantities are approximately 2π times the inner scale (l_0) and outer scale (L_0), respectively, of the turbulent irregularities in the medium. Turbulent fluctuations with scales between l_0 and L_0 lie within the so-called inertial subrange of turbulence and are generated by sources with scales greater than L_0 and viscously damped at scales smaller than l_0.

Radar half-wavelengths in the VHF and UHF bands ranging between roughly 5.0 to 0.05 meters typically span the inertial subrange of turbulent irregularities in the middle atmosphere.

The inner scale is given by $l_0 \equiv (\nu^3 / \epsilon_d)^{1/4}$, where ν is the kinematic viscosity and ϵ_d is the dissipation rate, and increases with height (Tatarskii, 1971). Figure 1, taken from Balsley and Gage (1980), shows the calculated height distribution of the minimum scale of turbulence, $\lambda_{min}/2\pi$, using standard atmospheric values for ν and expected values for ϵd based on radar observations. Balsley and Gage (1980) used various radar observations (solid circles) to generate the model curve. Direct in-situ balloon measurements of the inner scale (crosses in Figure 1) in the stratosphere by Barat (1982) agree to within an order of magnitude of the calculated values.

The maximum height of observed backscattered echoes from the neutral atmosphere by various radars is denoted by open squares in Figure 1. Backscatter measurements using the 1290 MHz radar formerly located at Chatanika, Alaska (presently located at Søndrestrømford, Greenland) by Balsley et al. (1977) were obtained to about 25 km, where one-half of the 0.23 m wavelength matches the minimum scale of turbulence predicted for that height. The maximum altitude of atmospheric echoes for the Arecibo 430 MHz radar is 31 km, although typically the upper limit is usually in the range 25-27 km (Woodman, 1980). For Arecibo, the maximum observed altitude is several kilometers less than the theoretically predicted 35 km altitude, where the radar half-wavelength of 0.35 meters matches λ_{min}. This difference is attributed to insufficient sensitivity of the Arecibo radar system (Woodman, 1980). Using the Jicamarca 49.92 MHz radar Woodman and Guillen (1974) and Fukao et al. (1979) observed backscattered echoes up to 35 km and 30 km, respectively, before the loss of radar sensitivity. The maximum observed height at VHF is considerably less than that predicted from turbulence theory. Our goal in this study is to determine whether this height limit at VHF can be increased.

All of the VHF and UHF radar half-wavelengths used for turbulent scatter studies in the neutral atmosphere are smaller than the outer scale of the turbulence. Outer scales of turbulence throughout the neutral atmosphere are predicted to be on the order of 10 meters (Woodman and Guillen, 1974; Van Zandt et al., 1978). Recent in-situ balloon measurements of the outer scale in

the stratosphere (Barat, 1982) are in the 10-30 meter range and agree well with predicted values (solid triangles in Figure 1). However, Yamanaka and Tanaka (1984) suggest that multiple "gust" layers with thicknesses on the order of 10's of meters are embedded within turbulent layers, which are a few hundred meters thick.

Numerous attempts to observe through the entire neutral atmosphere at VHF have been made starting with the pioneering work of Woodman and Guillen (1974) using the Jicamarca radar. Subsequent attempts by Fukao et al. (1979) using the Jicamarca radar, by Ruster et al. (1980) using the 53.5 MHz SOUSY radar, and Balsley (1983) using the 49.92 MHz Poker Flat radar did not yield a discernable atmospheric signal through the 35-55 km gap region. However, an earlier study by Balsley (1978), using the Jicamarca radar at full power and with the entire antenna area for maximum sensitivity, showed that an atmospheric signal in the 35-55 km region is detectable if sufficient signal averaging is employed. Figure 2 is a power profile of Balsley's results for a 49-minute averaging period. Thus, detectable signals from the gap region appear to be attainable if sufficient system sensitivity is available.

We report here results of a set of observations of atmospheric echoes through the entire neutral atmosphere using the Jicamarca radar at maximum sensitivity. The primary difference between these observations and those previously reported by Balsley (1978) is that the current experiment implemented a complementary coded-pulse compression scheme to increase the sensitivity of the radar system and to enhance signal detectability. The detectability of an atmospheric echo, which is measured by the ratio of signal power to the uncertainty of the noise power, is, as noted by Farley (1985), proportional to the average transmitter power, antenna area, number of coherently added received signals, and square root of the number of incoherently added powers or power spectra, and is inversely proportional to the effective noise temperature, receiver bandwidth, and range squared. The present experiment is an attempt to optimize the controllable parameters. The number of coherent integrations, which is limited by the product of the correlation time of the atmospheric medium (~.5 s) and the maximum pulse repetition

frequency (PRF) (~1 KHz) to avoid range aliasing from ionospheric echoes, is constrained to 100-200 integrations. Through pulse compression techniques, maximum transmitter duty cycle and average transmitter power are achieved while maintaining good height resolution. Phase coding, the pulse compression scheme used in the present experiment, yielded duty cycles and average transmitted powers 2-4 times that achieved by Balsley without coding. Finally, incoherent integration, done off-line in the present experiment, is accomplished until signal detectability is enhanced above the noise.

After discussing the operating and processing parameters of this experiment in the next section, we present in the following section the measured backscattered echoes. Subsequently we discuss the attainability and verifiability of echoes from the gap region.

Experimental Setup

The entire 50 MHz antenna at the Jicamarca Radio Observatory, Peru, was used on 21-22 January 1978 to obtain the present measurements. Pertinent operating and processing parameters are listed in Table 1. The four transmitter tubes were operated at their maximum obtainable peak power of 3 MW. The full antenna was used for transmission and reception on the same polarization. One polarization was phased to the on-axis position, which is directed to 1° off-vertical and utilizes the full effective antenna area. The other polarization was phased to the vertically pointing direction. Measurements were taken alternately for each polarization during different observation periods.

For pulse compression, three different phase coding schemes were implemented: uncoded, two-baud binary code, and four-baud binary complementary code. Complementary code sets, first proposed by Golay (1961), have the properties of linearity and perfect decoding. Perfect decoding is the property that the decoded waveform of the code sequence has zero range sidelobes. In the absence of transmitter and receiver imperfections and for a slowly moving target, when the two complements of the complementary code set are individually decoded and

subsequently summed together, the resultant correlation is perfect and compressed by 2N, where N is the number of bauds in the code. Furthermore, decoding of the complementary code set is a linear process, and so the order of implementation of decoding followed by coherent summing may be switched so as to reduce hardware processing requirements. The complementary code set (A, B), for the two-band code was (+ -, ++); for the four-band code (A = +++-, B + ++-+). In addition, the transmitted code sequence was alternately shifted by 180° to eliminate system DC biases, i.e., A, B, A, B, where $^{-}$ signifies the sign inverted form of the code. Using a baud length of 16.6 μs and an interpulse period of 1.3 ms, the resulting duty cycles were 1.3%, 2.6%, and 5.1% for the uncoded, 2-baud, and 4-baud codes, respectively. The 4-baud code measurements, for which the 5.1% duty cycle approaches the maximum duty cycle of the Jicamarca transmitters, fully utilized the 150-160 KW of average power. Backscatter measurements for each of the three codes were made during separate observation periods.

Upon reception the backscattered signals were detected in quadature and sampled every 2.5 km for a total of 40 heights. During on-line processing samples at each height were coherently added (100 times for coded pulses, 200 times for uncoded pulses) and saved on magnetic tape. During off-line analysis the samples were decoded, and power spectra were computed from the time series using standard Fast Fourier Transform (FFT) algorithms. The resulting 64 or 128 point power spectra were incoherently averaged between 10 and 40 times yielding a total integration period between 2.7 and 11 minutes.

Conventional treatment of the 0 Hz or DC bin by notch filtering the 0 Hz bin was inappropriate in this experiment since Doppler shifts of atmospheric echoes of a vertically pointing beam are very small and would be filtered out as well. Instead the following scheme was used. An incoherent average was accumulated from the average of power spectra at 0 Hz, i.e. the sum of squares of the real and imaginary output channels of the FFT calculations, and, for the same averaging period, a coherent average was accumulated for 0 Hz, i.e. the normalized square of summations of real and imaginary output channels of the FFT calculations. The

incoherent average is the contribution of power at 0 Hz from all sources: backscattered echo, system and cosmic noise, and ground clutter. Since the coherence times of atmospheric signals are short (< .5 second) and the noise is ideally white (i.e. uncorrelated between pulses), the coherent average at 0 Hz estimates the true DC, i.e. stationary, non-slowly varying contributions of 0 Hz. System DC was previously removed by the 180° flip between transmitted pulses. The remaining DC contributions are echoes from stationary objects. Hence, the residual difference between the incoherent and coherent averages is an estimate of the sum of atmospheric signal and noise at 0 Hz. This treatment is necessary since the small Doppler shifts and widths of the backscattered signals mean that the signal spectra are defined by just a few points around 0 Hz.

Results

Power spectra computed from measurements using uncoded pulses taken on 21 January 1978 are shown in Figure 3. The 128-point power spectra were incoherently integrated 40 times to yield an integration period of 11 min. The spectra are plotted for the first 37 heights and are normalized about the maximum peak for each spectrum. The lowest several heights display a very narrow spectral peak with little Doppler shift from 0 Hz. Although the ground clutter at 0 Hz has been subtracted out as much as possible, the spectra from 7.5 through 15.0 km may be not totally free of contaminating effects. Possible recovery delays in the receiver and the transmitter/receiver switch, and saturation during digitization by strong ground clutter can introduce biases into the lowest heights. For heights 22.5 through 37.5 km, the spectral peaks display a broader width with perceptible non-zero Doppler shift and are indicative of a backscattered atmospheric signal.

Above 35 km the noise level appears to increase because the strength of the normalized spectral peak of the backscattered signal decreases relative to the noise. Between 40.0 km and 57.5 km no atmospheric signal is discernable from the noise fluctuations. Thus, a gap in the discernable returned atmospheric signal exists in the profile of spectra for the uncoded pulses

between 40.0 and 57.5 km. An estimate of the noise level at each height, which is calculated from the mean of sixteen points total taken from the eight values at the extreme left and right, i.e. "wings", of the spectrum, is constant with height for the range 30.0 - 70.0 km, as expected. Hence, the loss of an atmospheric echo is attributed to the decrease in atmospheric signal strength to below the detectability threshold and not to an increase in the level of noise.

Above 60.0 km, an atmospheric signal is again discernable in the spectra with peaks that are broader and have larger Doppler shifts than those below the gap region. The increase in power and width is consistent with other observations at VHF and is attributed to enhanced scattering from neutral turbulence in the presence of a gradient in the index of refraction (Woodman and Guillen, 1974). The change in index of refraction is due in turn to the increasing presence of free electrons in the D region. Gravity waves, whose amplitudes grow exponentially with height, can produce at mesospheric heights the large vertical velocities observed. Above 85.0 km the spectral peaks of the backscattered signal broaden and become increasingly indistinguishable from the noise variations. At 90.0 km and above the equatorial electrojet is a prominent feature in the equatorial ionosphere. Since the coherence times of the electrojet echoes are considerably shorter than the coherent averaging times used in this experiment, the result is a broader, more noise-like spectrum.

A comparable height profile of computed power spectra, but for pulses coded with the 4-baud complementary code set, is shown in Figure 4. This profile was taken about one-half hour after the previous uncoded profile for a comparable 11 minute period. The number of incoherent integrations (= 20), is one-half that of the uncoded profile, since the two-part complementary code set effectively doubles the number of coherent additions compared to an uncoded pulse. Mean Doppler shifts for the uncoded (Figure 3) and coded (Figure 4) profiles are comparable below and above the 40.0 - 57.5 gap region. Differences in the mean Doppler shift between the two profiles can be attributed to short period gravity wave activity. In the 40.0 - 57.5 gap region, however, the profile of the coded pulses displays an identifiable peak. Although the

signal is not much above the noise level in the 40.0 - 50.0 km range, the signal peak is clearly discernable from the variability in the noise. Thus, the coding scheme has effectively raised the integrated signal above the noise level.

Besides increasing the average power, and therefore the effective peak power, by a factor of 4, pulse coding lengthens the transmitted pulse train from 2.5 km to 10.0 km. In the lowest range gates, this lengthening smears ground clutter over a wider range of gates. In Figure 4 the narrow peaked spectra with near-zero mean Doppler shift below 25.0 km suggests that contamination by ground clutter is present. The upper three range gates are not plotted since four consecutive range gates are required to decode a pulse train.

Profiles of the spectral measurements taken using the 2-baud complementary code were not made on the same day as the uncoded and 4-baud coded pulses. However, analysis of the 2-baud code measurements showed little difference from the uncoded measurements and hence the 2-band code do not exhibit a significant enhancement of signal sensitivity in the gap region as do the 4-baud codes.

Additional backscatter measurements using the 4-baud complementary code pulse scheme were taken on 22 January 1978 for two antenna pointing directions, vertical and 1° off vertical. In the 1° off vertical (the so called "on-axis" position) the antenna is phased for maximum efficiency. The efficiency for the on-axis position is 0.63; for the vertical position it is 0.51.

Spectra have been computed from the backscattered signals for both antenna positions. For each height, 64-point spectra were calculated and subsequently incoherently averaged 40 times for a total averaging period of 11 minutes. Profiles of the computed spectra from 17.5 to 95.0 km for the vertical and on-axis positions are plotted (triangular points connected by dashed curve) in Figures 5 and 6, respectively. Each spectrum is normalized to its maximum value. It should be noted that the two profiles were not taken simultaneously but are separated by about a 2-1/2 hour period. Signals are discernable in the "gap" region in both figures, but are clearly

somewhat stronger in Figure 6.

To provide estimates of signal and noise parameters for each computed spectrum, the following calculations have been performed. The "signal" portion of the DC bin of the spectrum has been estimated by subtracting the coherent average from the incoherent average of the 0 Hz bin. The level and variability of the noise have been estimated by calculating the mean and standard deviation of the "wings" of the spectrum, i.e. the outer eight points on both the extreme left and extreme right of the spectrum. Subsequently, after the noise level has been subtracted out, the spectrum was fitted to a Gaussian by least-squares method. Estimates of the signal power, mean Doppler shift, and Doppler width correspond to the first 3 moments of the Gaussian, respectively. From these signal parameter estimates, a best-fit spectrum from the estimated signal and noise parameters has been constructed. The best-fit curves are plotted as the solid curves in profiles of spectra in Figures 5 and 6.

The spectra of Figures 5 and 6, which are similar to those of Figure 6.5, are typical of those generally observed in the stratosphere and mesosphere at Jicamarca. Spectra in the lower stratosphere are narrow in width and show small Doppler velocities in both the vertical and nearly vertical direction. While the signal strength drops off as the altitude increases, the signal peaks in the 35-55 km region are detectable though at some heights are barely above the noise fluctuations. An increase in signal power occurs above 55 km due to the increasing concentration of free electrons in the lower ionosphere. At mesospheric heights, the broader spectra are typical of those due to turbulent scatter. However, in the off-vertical profile (Figure 6), stronger and narrower spectral peaks with larger Doppler shifts are observed between 70.0 and 80.0 km, in addition to the weaker and broader peaks that are associated with turbulent scatter.

The source of these stronger peaks is not clear. Scattering from meteor trails at VHF is characterized by the occurrence of nearly identical and narrow peaks over several contiguous heights and by rapid fading times (Rottger et al., 1979). VHF radar observations of meteor

scatter over Poker Flat indicate that meteor echoes typically last one second or less, usually occupying only one range gate, and are distributed ±10 km around a median height of 93 km (Avery et al., 1983). The strong peaks in Figure 6 are over a height range of 70.0-80.0 km, which is considerably lower than the height ranges associated with meteor scatter. Furthermore, the 11 minute averaging period of the present observations is much longer than the coherence time of meteor echoes. On the other hand, the sidelobe patterns of the Poker Flat and Jicamarca antennas are different, as are, of course, the latitudes. Alternatively, these strong peaks could be an echo from a satellite at higher altitudes, which has been range aliased. However, the transient time of a satellite through the antenna beam is 1 - 2 minutes or less.

Results of the determination of signal parameters by a least-squares fit to spectra in Figures 5 and 6, are presented in the next several figures. Figure 7 shows for both the vertical and 1° off vertical beams the signal-to-noise (S/N) as a function of height, where the signal is taken as the peak of the fitted spectrum and the noise level is obtained by the method previously described. For both beams the S/N curves drop off roughly exponentially reaching a minimum at 45.0 km. The rate of decrease in S/N is 1.25 dB per km between 17.5 and 27.5 km and the rate accelerates to 2.0 dB per km in the next 10 km. For the Jicamarca radar antenna, the crossover from the near to far fields occurs at about 20 km and could account for any apparent changes in received power. Between 40.0 and 50.0 km the S/N ratio slowly decreases to a minimum at 45.0 km and then slowly begins to increase with height. From 50 to 60 km the ratio rapidly increases at a rate of 2.0 dB per km. While the S/N profiles for the vertical and 1° off vertical beams coincide well up through 60 km, the profiles diverge above there. The wide variation from 60.0 to 90.0 km is attributable to the variability in turbulent backscatter in the mesosphere. Furthermore, the least-squares fitting routine locked onto the strong, secondary peak in the 1° off vertical beam between 70.0 and 80.0 km, which resulted in significant deviations in signal power, Doppler shift, and width from the other heights and the other beam. These observations are in general in accord with other observations of turbulent backscatter from the mesosphere

(Rottger et al., 1979).

Profiles of signal detectability, where detectability (S/δN) is defined as the ratio of the signal power (i.e. peak of the fitted spectrum) to the uncertainty (standard deviation) of the noise, are shown for the vertical and on-axis directions in Figure 8. In Figure 8, 0 dB represents a barely detectable signal, and it is clear that both curves are above this level at all altitudes. The detectability drops off at 1.5 dB/km between 17.5 and 27.5 km and the drop-off rate increases to 2.0 dB/km between 27.5 and 37.5 km. The detectability is nearly constant and on the order of a few dB between 40.0 and 50.0 km. From 50.0 to 60.0 km the detectability rapidly increases. Above 60.0 km the detectability profiles of the two beams do not correlate as well as below 60.0 km. Since δN is proportional to N for random noise, the profiles of Figures 7 and 8 should be nearly identical in shape. However, estimates of δN and N from the spectra may differ from "true" values and thus explain any apparent differences. The erratic and variable nature of the profiles above 60.0 km is due in part to the temporal variability of turbulent bursts in the mesosphere (Harper and Woodman, 1977).

Figure 9 shows profiles of the line-of-sight velocity. Amplitudes are on the order of .5 m/s or less for the vertical beam. Amplitudes in the on-axis beam are somewhat larger, in part due to the projection (sin 1°) of horizontal velocities onto the beam. The strong deviations in the velocity profile in the off-vertical beam between 55.0 and 57.5 km and between 70.0 and 80.0 km are due to the presence of strong secondary peaks. These observed vertical and near vertical velocities are 50% smaller than those previously observed at Jicamarca by Woodman and Guillen (1974) and Harper and Woodman (1977).

Discussion

A comparison of the profiles of spectra for the uncoded and the 4-baud complementary coded pulses indicates that the coding scheme effectively increases the sensitivity of the radar to the point that echoes are received from the gap region. Indeed, these are the first Doppler spectra by VHF radar through the entire neutral atmosphere to include the gap region. However, these results immediately give rise to two questions: How verifiable are these measurements? Why is this experiment successful in obtaining backscattered signals from the gap region when other experimental attempts have failed?

In answer to the second question, the reason is that previous attempts at Jicamarca and elsewhere did not have the system sensitivity that the Jicamarca radar had during the present experiment. Table 6.2 lists the average power-aperture products used in attempts to obtain radar backscatter measurements through the entire atmosphere. The combination of the large average power produced by a high duty cycle and a large peak power, and the large antenna area of the Jicamarca radar yielded for the present experiment an average power-aperture exceeding by a factor of 2 or more those of previous experiments. Balsley (1978) found that, using an average power of one-half that of the present experiment, echo power above the noise level could be achieved after averaging 49 minutes. In the present experiment the attainability of Doppler signals after an 11-minute averaging period indicates that beyond a threshold of 10^{10} W-m^2 for the average power-aperture, backscattered echoes at 50 mHz can be obtained from throughout the entire daytime atmosphere.

The shorter integration time of the present experiment is attributable in part to the method of noise estimation. Balsley (1978) estimated a cosmic noise level by interspersing the data records of backscattered echoes with noise records, when data were recorded with the transmitter off. This approach for establishing the noise level has two problems: (1) the cosmic noise level varies on a time scale of ~4 minutes as distant radio sources pass through the narrow antenna

beam, and (2) the noise level is a function of time after transmitter pulse due to receiver recovery. In addition the noise cycle wastes time that could otherwise be used for further integration of the signal. As done in this experiment the procedure of estimating the noise level from the wings of the spectrum is self-consistent, includes the effects of noise variability and the contributions from various noise sources, and maximizes the transmitter duty cycle.

The first question could be most easily answered by a cornerstone in scientific inquiry: repeat the experiment. Unfortunately, the capabilities of the Jicamarca radar diminished substantially after this experiment. Recent refurbishment of two of the transmitters at Jicamarca has restored the capabilities of the system to something approaching those of 1978. A repeat of the present experiment should be feasible in the near future and would confirm the validity of the present results.

If these observed spectra are not due to atmospheric echoes, what might be the source? There are several possibilities. First, ground clutter could persist beyond the observed 15 to 20 km range gates into more distant ranges. However, the observed spectra in the gap region do not resemble the narrow, zero-Doppler shift spectra of ground clutter at lower altitudes. A mapping for ground clutter was undertaken in 1982 using a directional Yagi antenna pointing horizontally. The 8-element Yagi antenna used had a forward gain of ~11 dB, while the gain of the first sidelobe relative to the mainlobe of the full Jicamarca array was -14 dB. For radar applications (send and receiver) these values are doubled. In addition, the horizontal sidelobe gain of the Jicamarca array is even lower than the first sidelobe. The mapping with the Yagi antenna did not reveal any significant ground clutter from mountain peaks beyond 25 km. The lack of ground clutter beyond 25 km as observed by the Yagi with enhanced directivity in the horizontal assures us that the echoes observed with the big Jicamarca array for heights above 25 km are free of ground clutter.

Another possibility is that the observed signals in the gap region are from other VHF transmitters ducted through the atmosphere. While plausible, since VHF signals could be ducted along atmospheric waveguides, this would be too coincidental to occur within a fraction of a Hertz from the 49.920 MHz operating frequency. One would expect other VHF signals to have a wider bandwidth than the observed narrow peaked atmospheric echoes. Furthermore, the transmitted complementary coded pulses are subsequently decoded by the appropriate matched filter. Other VHF signals would be unmatched to the decoding process, or if at 49.920 MHz, filtered to zero by the 180° flip.

We have exercised great care in ascertaining that these measurements have been properly decoded and processed. We are confident that our observed spectra at all heights are due to atmospheric backscatter, and we believe that radar probing is possible through the gap region.

The observed profiles of signal detectability support the conclusion that valid atmospheric echoes have been received in several respects. First, as noted above, the signal detectability is proportional to the square root of the number of incoherently averaged spectra. We have compared the detectability for spectra incoherently averaged 30 times to the detectability of spectra incoherently averaged 10 times. The resulting ratio of detectabilities for the profile is in the range of 1.5-2.0 which compares reasonably well to the predicted value of the square root of 3 or 1.7.

Second, Balsley and Gage (1981) have proposed a model of backscattering of VHF transmissions by horizontally stratified refractivity structures in clear air. The model predicts a drop off in VHF power profiles at the rate of 1.9 dB/km in the height range of 20-50 km. The observed decrease in power for the present experiments is 1.25 dB/km between 17.5 and 27.5 km and 2.0 dB/km between 27.5 and 37.5 km, values which are in good agreement with the model. A much smaller drop off in signal power is observed in the 40-50 km region and differs significantly from the Balsley and Gage model. The difference between the observed and model

curves at the upper heights remains to be explained.

Third, the enhanced antenna efficiency of the on-axis (1° off vertical beam) compared to the vertical beam is .9 dB. Below 30 km the signal detectability profiles for the two beams coincide. Above the 30 km the signal detectability of the on-axis beam is enhanced 1-2 dB over the vertical beam. The increase in antenna efficiency of the on-axis beam is counteracted to some degree by a decrease in reflected power due to specularity of VHF backscatter from the stratosphere as first observed by Gage and Green (1978) and Rottger and Liu (1978). Fukao et al. (1979) observed a drop off in power of stratospheric echoes at Jicamarca by a factor of 2-10 between quasi-vertical and 3.45° off-vertical beams. In the present experiment the small difference in pointing angles appears to be outweighed by the enhanced antenna efficiency. However, the possible occurrence of a favorable tilt for a specular reflection surface (e.g. leewaves) cannot be eliminated.

If VHF radars are capable of observing through the entire neutral atmosphere, is the cost of operating a radar rated at a power-aperture of 10^{10} W-m^2 or more worth it? Two reasons support such an effort. First, MST radars offer the potential of becoming the first technique to observe winds through the entire 0-100 km altitude region. Moreover, the MST radar technique is capable of observing winds in the 40-55 km region, where few other remote sensing techniques operate. The occurrence of turbulent irregularities in the upper stratosphere, which is considered to be inherently stable, gives rise to the questions of how these irregularities originate in this region and how they influence transport of trace constituents. Second, the MST radar technique is capable of measuring directly vertical velocities. Vertical motions are of great importance since they relate to vertical transport of trace constituents in the atmosphere. Further confirmation of VHF backscatter echoes from the 40-55 km gap region in the atmosphere is necessary, however, before the implementation of a whole atmospheric wind profile network becomes reality.

Conclusions

We have observed VHF radar signals backscattered through the entire neutral atmosphere from 17.5 to 90.0 km. Our results indicate that a minimum average power-aperture threshold of 10^{10} W-m^2 is required for MST radar systems operating near 50 MHz to observe throughout this region including the 35.0-55.0 km gap region.

References

Avery, S. K., A. C. Riddle, and B. B. Balsley, 1983: The Poker Flat, Alaska, MST radar as a meteor radar. *Radio Sci.*, **18**, 1021-1027.

Balsley, B. B., 1978: The use of sensitive coherent radars to examine atmospheric parameters in the height range 1-100 km. *Preprints, 18th Conf. on Radar Meteorology*, (Atlanta) AMS, Boston, 190-193.

Balsley, B. B., 1983: Poker Flat MST radar measurements of winds and wind variability in the mesosphere, stratosphere, and troposphere. *Radio Sci.*, **18**, 1011-1020.

Balsley, B. B., and K. S. Gage, 1980: The MST radar technique: potential for middle atmospheric studies. *Pure Appl. Geophys.*, **118**, 452-493.

Balsley, B. B., N. Cianos, D. T. Farley, and M. J. Baron, 1977: Winds derived from radar measurements in the Artic troposphere and stratosphere. *J. Appl. Meteorology*, **16**, 1237-1239.

Barat, J., 1982: Some characteristics of clear-air turbulence in the middle stratosphere. *J. Atmos. Sci.*, **39**, 2553-2564.

Farley, D. T., 1985: On-line data processing techniques for MST radars. *Radio Sci.*, **20**, 1177-1184.

Fukao, S., T. Sato, S. Kato, R. M. Harper, R. F. Woodman, and W. E. Gordon, 1979: Mesospheric winds and waves over Jicamarca on May 23-24, 1974. *J. of Geophys. Res.*, **84**, 4379-4386.

Gage, K. S., and J. L. Green, 1978: Evidence of specular reflection from monostatic VHF radar observations of the stratosphere. *Radio Sci.*, **13**, 991-1001.

Golay, M. J. E., 1961: Complementary series. *IEEE Trans. Inf. Theory*, **IT-7**, 82-87.

Harper, R. M., and R. F. Woodman, 1977: Preliminary multiheight radar observations of waves and winds in the mesosphere over Jicamarca. *J. of Atmos. and Terr. Phys.*, **39**, 959-963.

Rottger, J., and C. H. Liu, 1978: Partial reflection and scattering of VHF radar signals from the clear atmosphere. *Geophys. Res. Lett.*, **5**, 357-360.

Rottger, J., P. K. Rastogi, and R. F. Woodman, 1979: High-resolution VHF radar observations of turbulence structures in the mesosphere. *Geophys. Res. Lett.*, **6**, 617-620.

Ruster, R., P. Czechowsky and G. Schmidt, 1980: VHF-radar measurments of dynamical processes in the stratosphere and mesosphere. *Geophys. Res. Lett.*, **7**, 999-1002.

Tatarskii, V.I., 1971: *The effects of the turbulent atmosphere on wave propagation*, NTIS TT-68-50464, 470pp.

VanZandt, T. E., 1982: A universal spectrum of buoyancy waves in the atmosphere. *Geophys. Res. Lett.*, **9**, 575-578.

Woodman, R. F., 1980: High-altitude resolution stratospheric measurements with the Arecibo 430-MHz radar. *Radio Sci.*, **15**, 417-422.

Woodman, R. F., and A. Guillen, 1974: Radar observations of winds and turbulence in the stratosphere and mesosphere. *J. Atmos. Sci.*, **31**, 493-503.

Yamanaka, M.D. and H. Tanaka, 1984a: Multiple gust layers observed in the middle stratosphere. *Dynamics of the Middle Atmosphere*, ed. J. R. Holton and T. Matsuno, Boston: D. Reidel, 117-140.

Figure Captions

Figure 1 Curve of minimum scale of turbulence λ_{min} ($\equiv 5.91_0$) versus height calculated from values of kinematic viscosity for the standard atmosphere and typical values of ϵ_d expected at different altitudes [after *Balsley and Gage, 1980*]. Crosses and solid triangles indicate direct balloon measurements of inner and outerscales, respectively, in the stratosphere by Barat (1982). Solid circles are estimates of λ_{min} based from several different radar measurements. Open squares indicate maximum height of observations of backscattered signals from the neutral atmosphere for three different radar frequencies.

Figure 2 Height profile of received power averaged over a 49-minute period obtained using the VHf radar at Jicamarca Radio Observatory in Peru. Error bars below 20 km arise from matching different profiles. Data points at about 42 km and 52 km are approximate and indicate maximum possible echo power [after *Balsley, 1978*].

Figure 3 The power spectra for uncoded pulses for the height range 7.5-97.5 km. Antenna was directed to 1° off vertical. Note the lack of a discernable signal in the 40.0-57.5 km region for the 11 minute integration period.

Figure 4 Computed power spectra for 4-baud complementary code pulses for the height range 7.5-97.5 km. The antenna was pointed 1° off vertical. Profile was taken 29 minutes after the uncoded profile of Figure 4 and shows an identifiable peak in the Doppler spectra through the 40.0-57.5 km region.

Figure 5 Computed power spectra (triangles connected by dashed curve) and least-squares fit of spectra to a Gaussian (solid curve) for vertically pointing beam.

Figure 6 Computed power spectra (triangles connected by dashed curve) and least-squares fit of spectra to a Gaussian (solid curve) for on-axis (1° off vertical) beam.

Figure 7 Height profiles of signal-to-noise in dB for vertical and 1° off vertical beams.

Figure 8 Height profile of signal detectability (signal-to-noise variance) in dB for vertical and 1° off vertical beams.

Figure 9 Radial Doppler velocity versus height for vertical and 1° off vertical beams.

Table 1

Jicamarca Radio Observatory
Operating and Processing Parameters for
Atmospheric Power Spectra Profiles

Transmitter:	Frequency	49.920 MHz
	Power	3.0-3.3 MW (Peak)
		160-170 KW (Average)
	Baud Width	16.7 μSec.
	Inter-Pulse Period	1.3 mSec.
Antenna:	Area (fill antenna)	8.4×10^4 meters^2
	Beamwidth	1°
	Pointing Directions	1. Vertical
		2. On-Axis (1° South of Vertical)
	Polarization	Linear
Pulse Coding:	Single Uncoded Pulse	
	2-Baud Complementary Code	
	4-Baud Complementary Code	
Processing:	Coherent Averaging	100 Pulses (Uncoded)
		200 Pulses (Coded)
	Spectra (FFT)	64 OR 128 Points
	Incoherent Averaging	40 Spectra (Uncoded)
		20 Spectra (Coded)
	Total Averaging Time	11-12 min.
	DC Elimination	180° Flip & Coherent Subtraction

Table 2

Power-Aperture Products of MST Radar Observations

Observation	Average Power-Aperture ($W\text{-}m^2$)
Woodman and Guillen, 1974	3.9×10^9
Balsley, 1978	5.3×10^9
Balsley et al., 1979	2.6×10^9
Fukao et al., 1979	2.2×10^9
Rottger et al., 1979	2.0×10^7
Ruster et al., 1980	2.2×10^7
This experiment:	
- no code	3.2×10^9
- 4-baud code	1.4×10^{10}

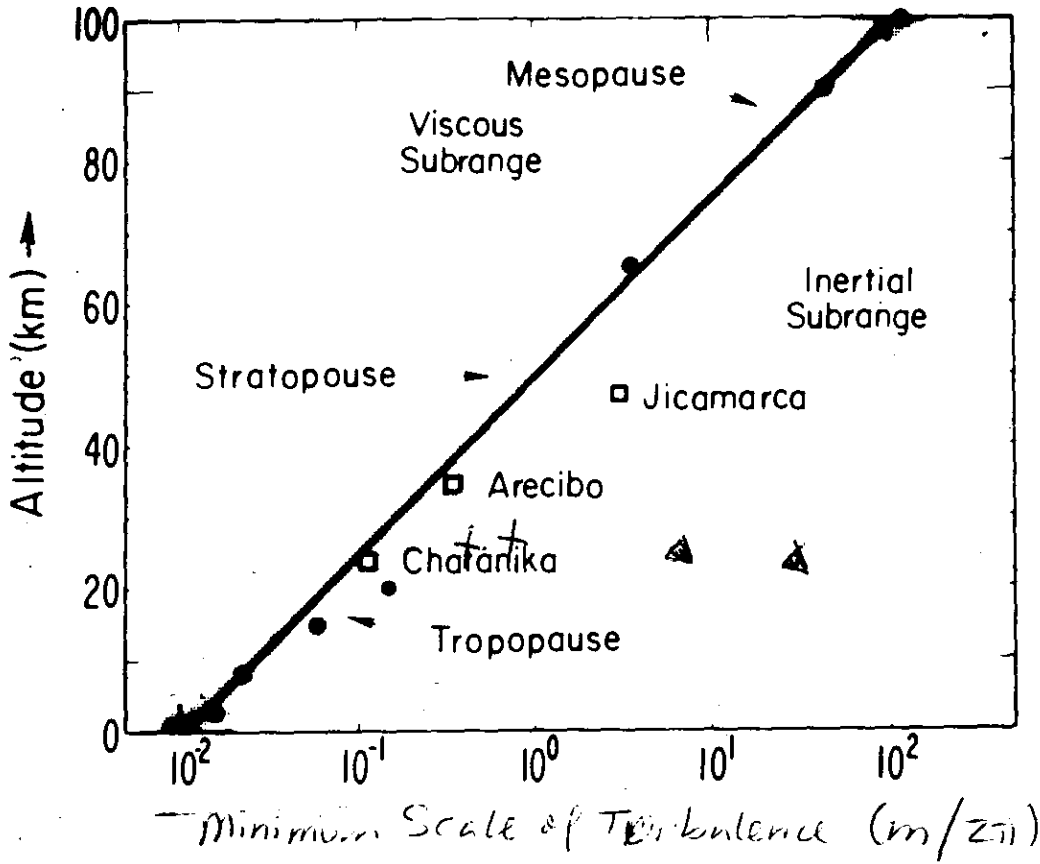
100
80
60
40
20
0
Altitude (km)
Mesopause
Viscous
Subrange
Inertial
Subrange
Stratopouse
Jicamarca
Arecibo
Chatanika
Tropopause
10^{-2}
10^{-1}
10^{0}
10^{1}
10^{2}
Minimum Scale of Turbulence (m/2π)

Figure 1

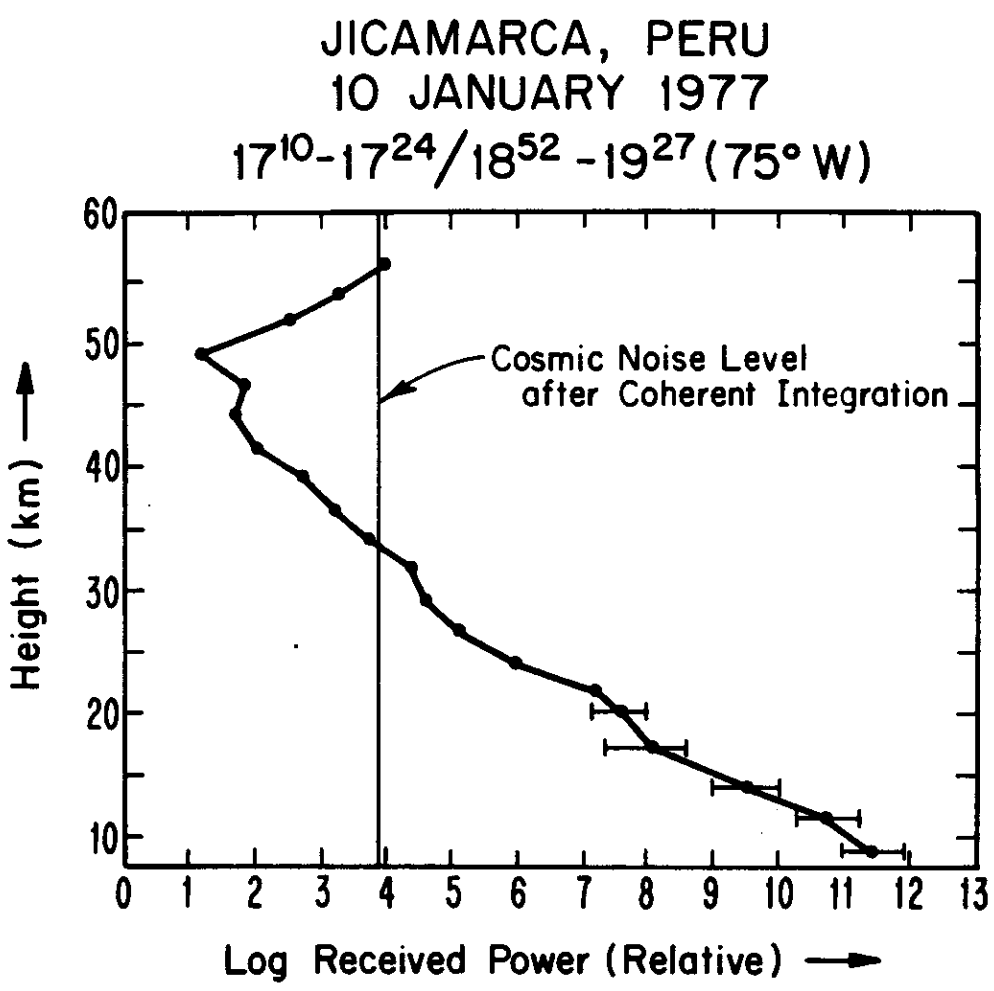
JICAMARCA, PERU
10 JANUARY 1977
17^10-17^24/18^52-19^27 (75° W)
Cosmic Noise Level
after Coherent Integration
Height (km)
60
50
40
30
20
10
0
1
2
3
4
5
6
7
8
9
10
11
12
13
Log Received Power (Relative)

F[illegible] 2

JICAMARCA RADIO OBSERVATORY

21 JANUARY 1978 15:57:00 - 16:08:05 LT

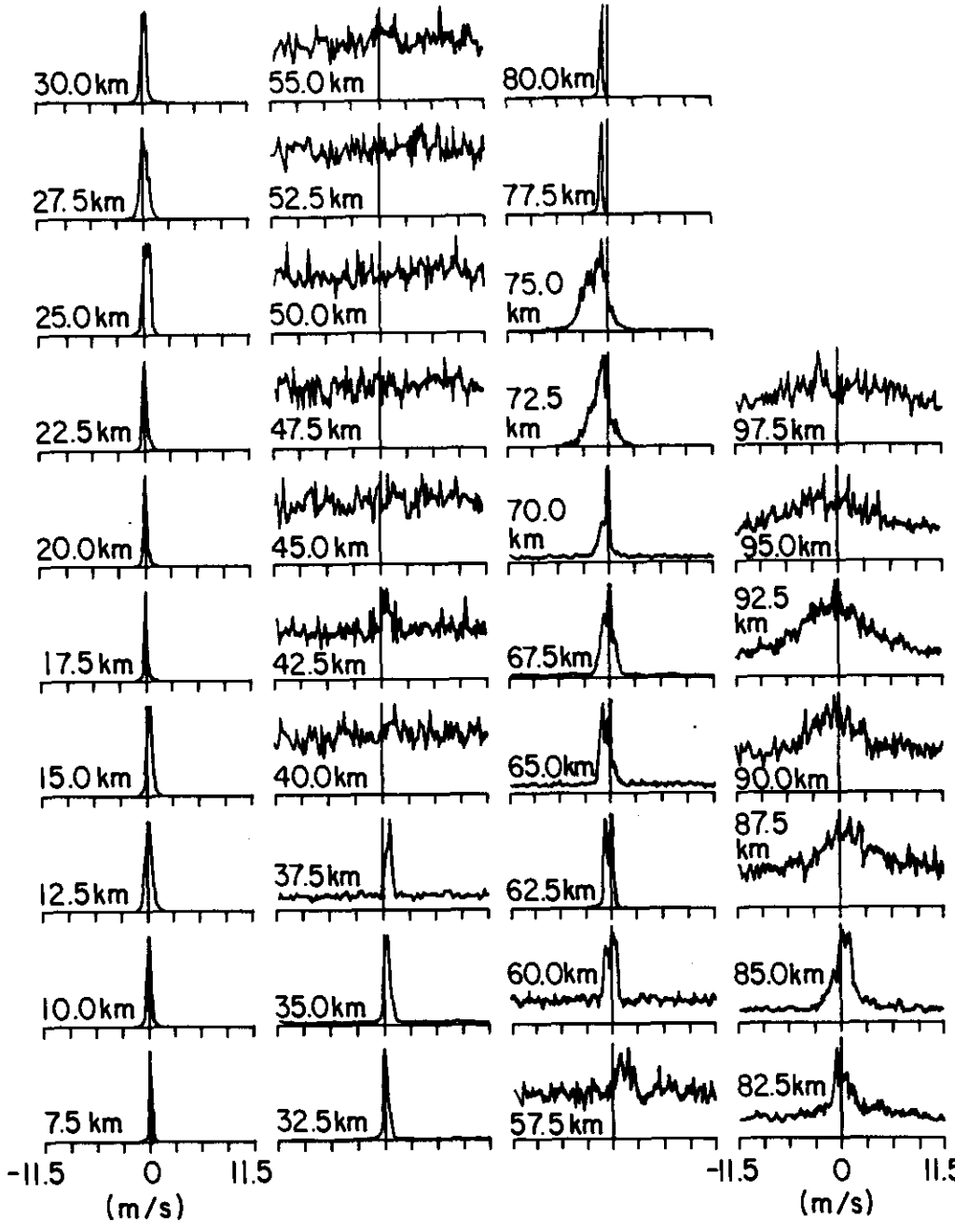

NO CODE 128 POINT FFT 40 INCOHERENT AVERAGES

JICAMARCA RADIO OBSERVATORY

21 JANUARY 1978 16:37:00 - 16:48:05 LT

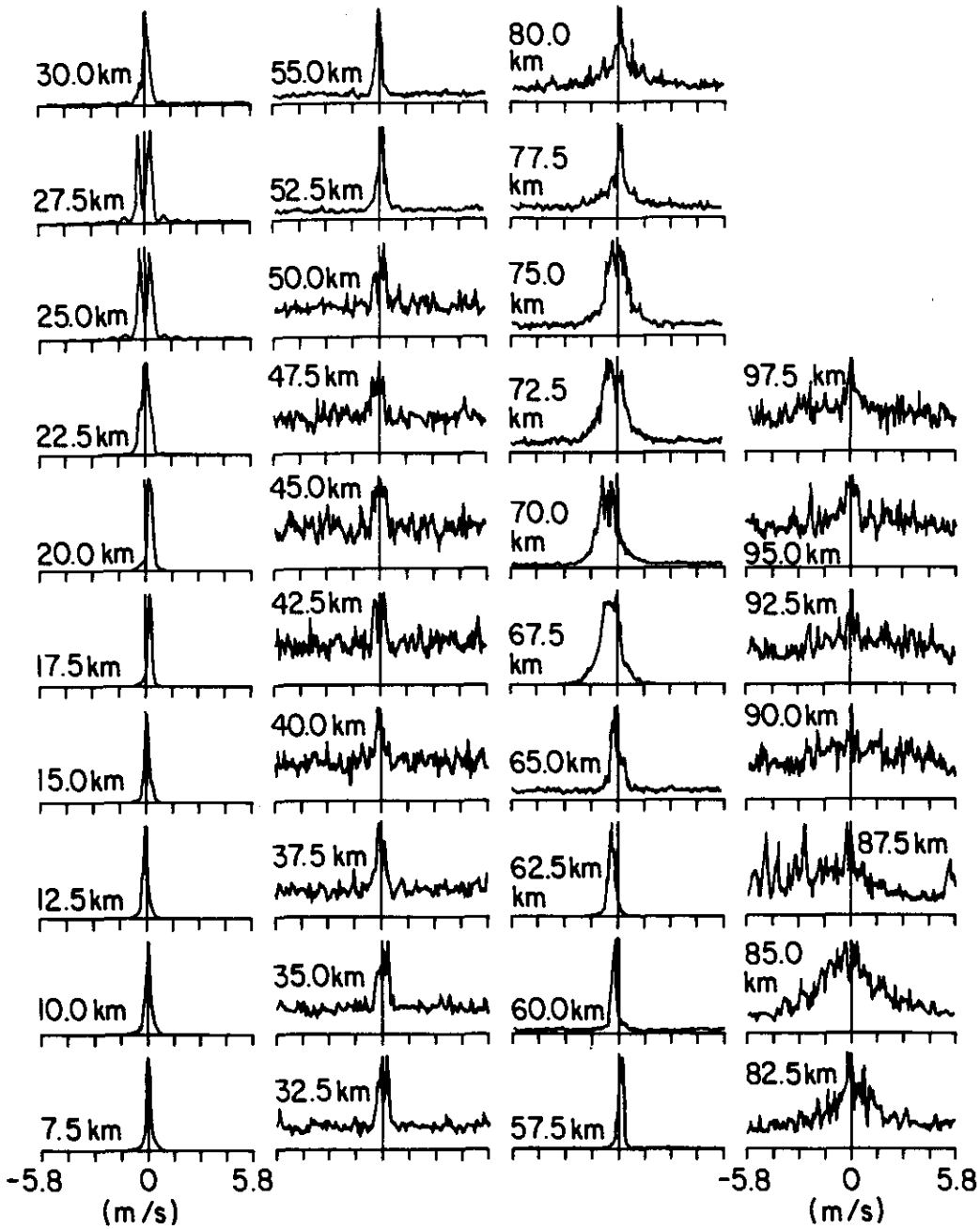

4 BAUD CODE 128 POINT FFT 20 INCOHERENT AVERAGES

Figure 4

JICAMARCA RADIO OBSERVATORY

22 JANUARY 1978 18:12:00 - 18:23:05 LT

VERTICAL

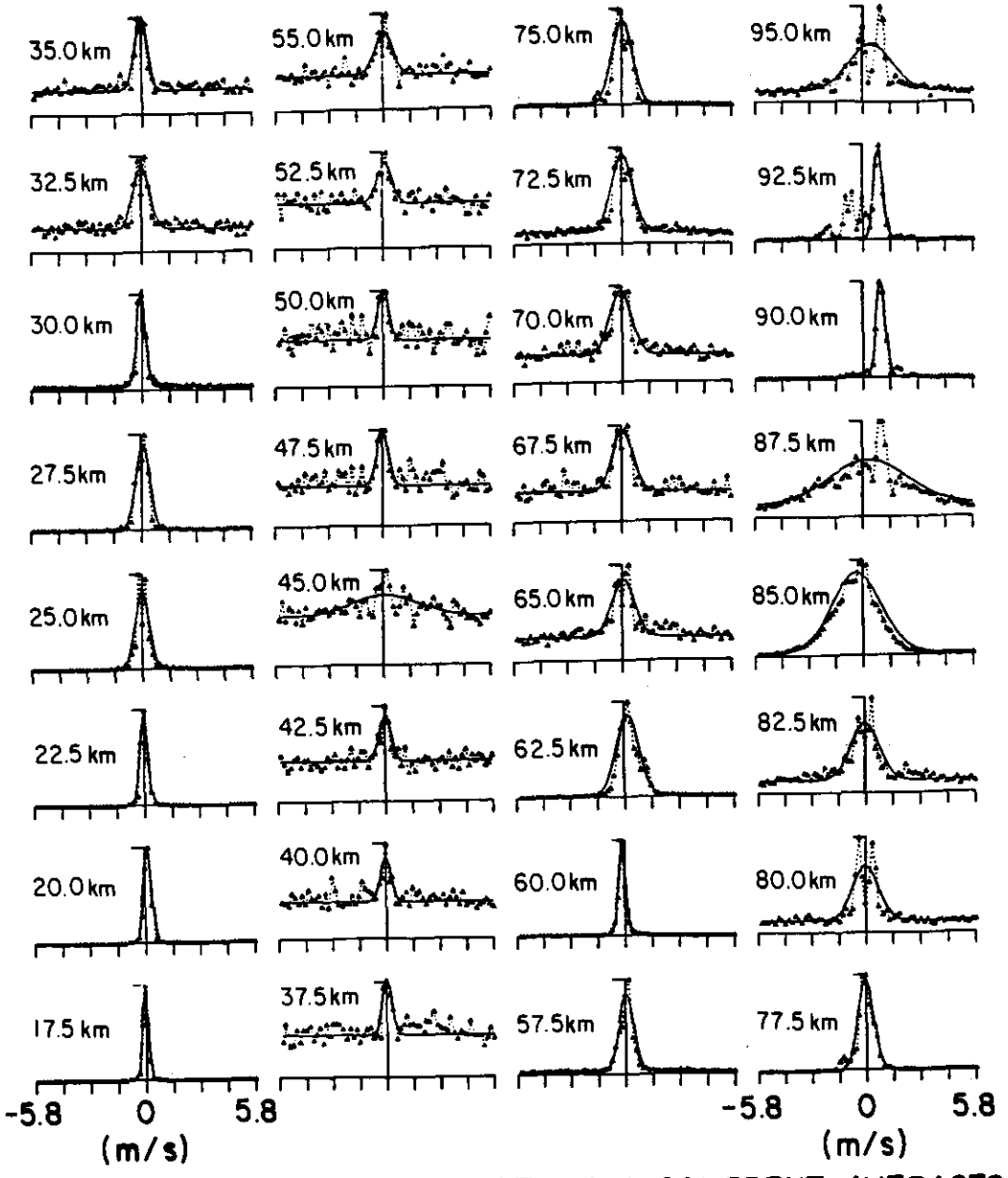

4 BAUD CODE 64 POINT FFT 40 INCOHERENT AVERAGES

• Computed Power Spectra

— L.S. Fit to Spectra

JICAMARCA RADIO OBSERVATORY

22 JANUARY 1978 17:37:00 - 17:48:05 LT

1° OFF VERTICAL

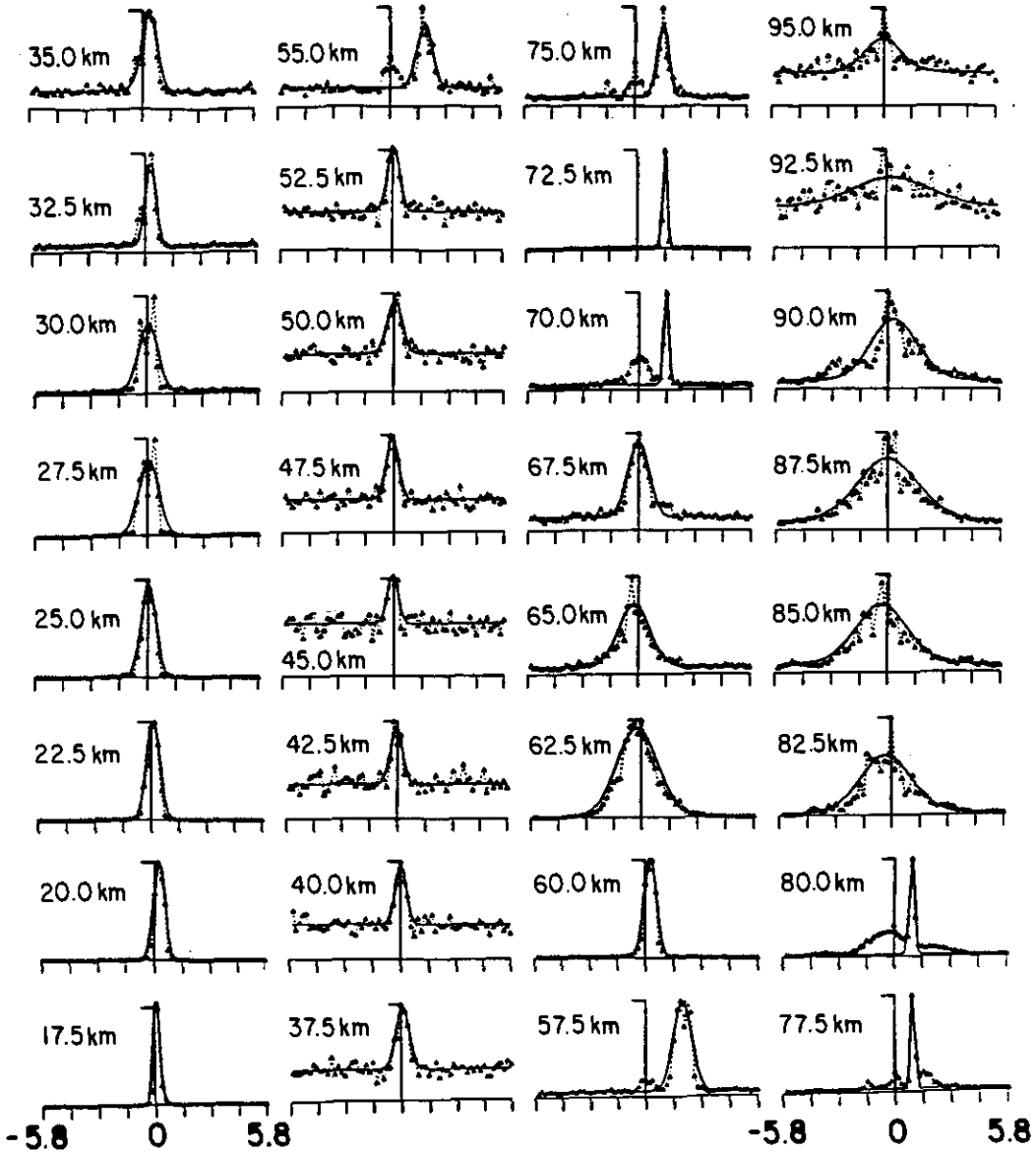

4 BAUD CODE 64 POINT FFT 40 INCOHERENT AVERAGES

▲ Computed Power Spectra

— L.S. Fit to Spectra

Figure 6

JICAMARCA RADIO OBSERVATORY

22 JANUARY 1978

1° OFF VERTICAL - 17:37:00 - 17:48:05 L.T.

VERTICAL - 18:12:00 - 18:23:05 L.T.

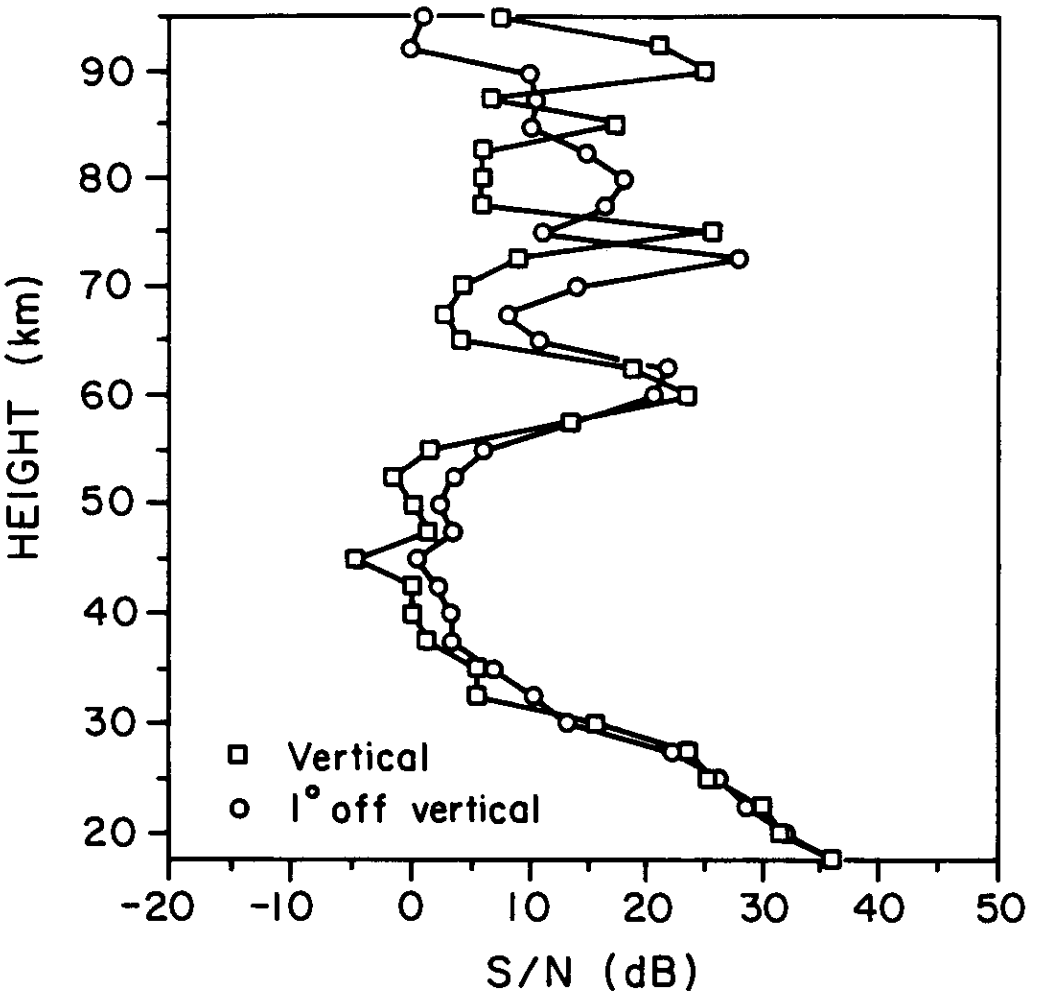

Figure 7

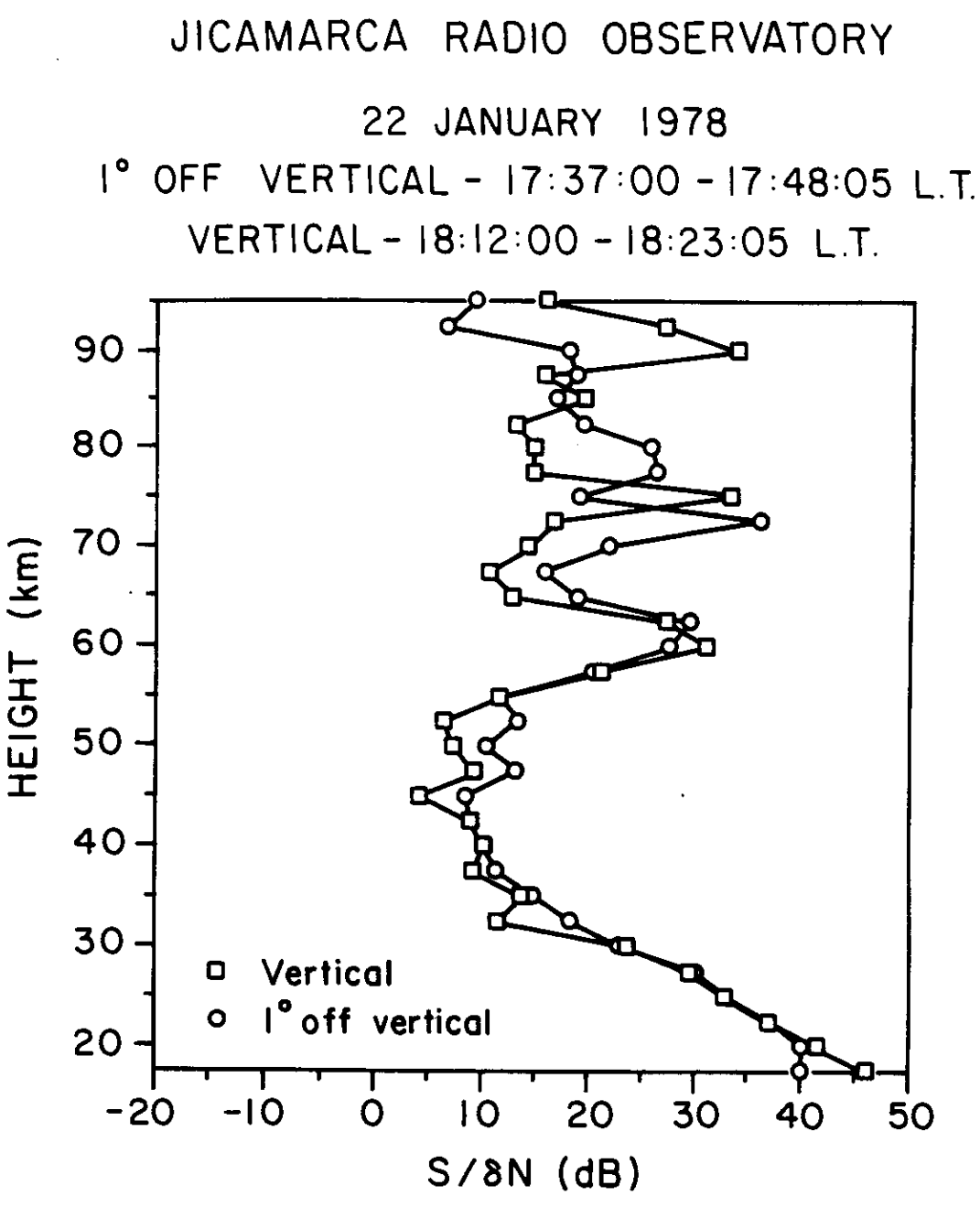
JICAMARCA RADIO OBSERVATORY
22 JANUARY 1978
1° OFF VERTICAL - 17:37:00 - 17:48:05 L.T.
VERTICAL - 18:12:00 - 18:23:05 L.T.
HEIGHT (km)
90
80
70
60
50
40
30
20
-20
-10
0
10
20
30
40
50
S/δN (dB)
Vertical
1° off vertical

Figure 8

JICAMARCA RADIO OBSERVATORY

22 JANUARY 1978

1° OFF VERTICAL - 17:37:00 - 17:48:05 L.T.

VERTICAL - 18:12:00 - 18:23:05 L.T.

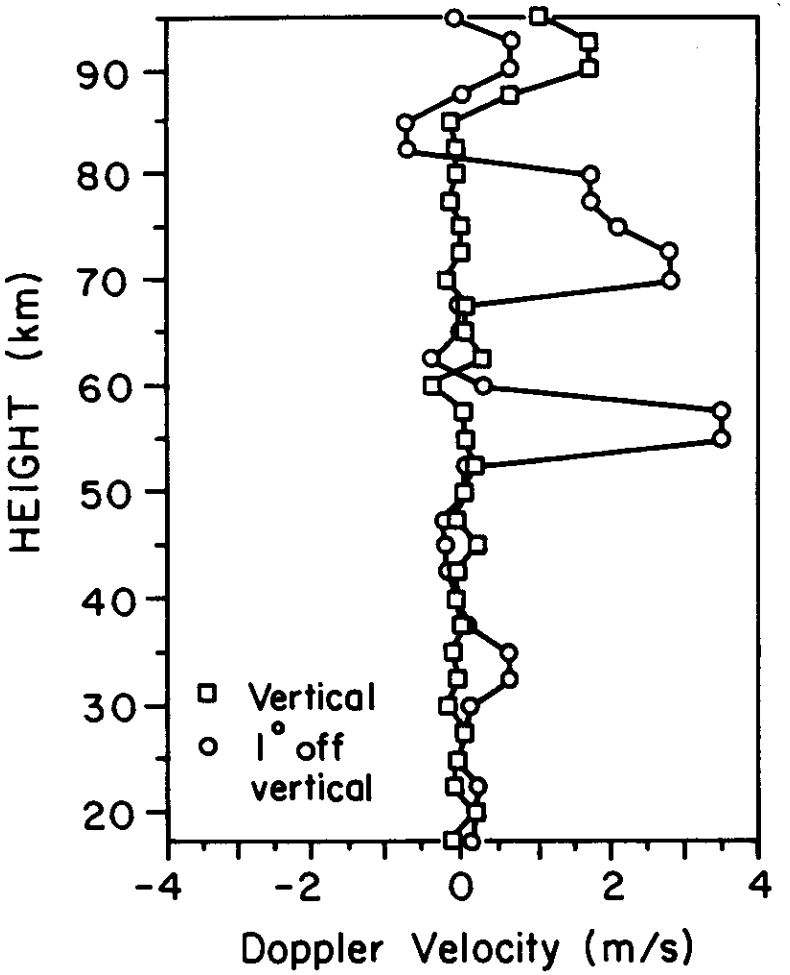

Figure 9